

# 1 Rainfall threshold calculation for debris flow early 2 warning in areas with scarcity of data

3 Hua-li Pan <sup>1, 2</sup>, Yuan-jun Jiang <sup>1, 2, ✉</sup>, Jun Wang <sup>3</sup>, Guo-qiang Ou <sup>1, 2</sup>

4 ✉ Corresponding author's e-mail: yuanjun.jiang.civil@gmail.com

5 <sup>1</sup> Key Laboratory of Mountain Hazards and Earth Surface Process, Chinese Academy of Sciences, Chengdu  
6 610041, China

7 <sup>2</sup> Institute of Mountain Hazards and Environment, Chinese Academy of Sciences, Chengdu 610041, China

8 <sup>3</sup> Guangzhou Institute of Geography, Guangzhou 510070, China

9 **Abstract:** Debris flows are one of the natural disasters that frequently occur in mountain ar-  
10 eas, usually accompanied by serious loss of lives and properties. One of the most used ap-  
11 proaches to mitigate the risk associated to debris flows is the implementation of early warning  
12 systems based on well calibrated rainfall thresholds. However, many mountainous areas have  
13 little data regarding rainfall and hazards, especially in debris flow forming regions. Therefore,  
14 the traditional statistical analysis method that determines the empirical relationship between  
15 rainstorm and debris flow events cannot be effectively used to calculate reliable rainfall  
16 thresholds in these areas. After the severe Wenchuan earthquake, there were plenty of dipos-  
17 its deposited in the gullies which resulted in lots of debris flow events subsequently. The trig-  
18 gering rainfall threshold has decreased obviously. To get a reliable and accurate rainfall  
19 threshold and improve the accuracy of debris flow early warning, this paper developed a  
20 quantitative method, which is suit for debris flow triggering mechanism in meizoseismal areas,  
21 to identify rainfall threshold for debris flow early warning in areas with scarcity of data based  
22 on the initiation mechanism of hydraulic-driven debris flow. First, we studied the characteris-  
23 tics of the study area, including meteorology, hydrology, topography and physical characteris-  
24 tics of the loose solid materials. Then, the rainfall threshold was calculated by the initiation  
25 mechanism of the hydraulic debris flow. **The comparison with other models and with alter-**  
26 **nate configurations demonstrates that the proposed rainfall threshold curve is a function of**

27 the antecedent precipitation index (*API*) and 1-h rainfall. To test the proposed method, we se-  
28 lected the Guojuanyan gully, a typical debris flow valley that during the 2008-2013 period  
29 experienced several debris flow events and that is located in the meizoseismal areas of Wen-  
30 chuan earthquake, as a case study. The comparison with other threshold models and with  
31 configurations shows that the selected approach is the most promising to be used as a starting  
32 point for further studies on debris flow early warning systems in areas with scarcity of data.

33 **Keywords:** Debris flow; rainfall threshold curve; rainfall threshold; areas with scarcity of  
34 data

## 35 **1 Introduction**

36 Debris flow is rapid, gravity-induced mass movement consisting of a mixture of water,  
37 sediment, wood and anthropogenic debris that propagate along channels incised on mountain  
38 slopes and onto debris fans (Gregoretti et al., 2016). It has been reported in over 70 countries  
39 in the world and often causes severe economic losses and human casualties, seriously  
40 retarding social and economic development (Imaizumi et al., 2006; Tecca and Genevois, 2009;  
41 Dahal et al., 2009; Liu et al., 2010; Cui et al., 2011; McCoy et al., 2012; Degetto et al., 2015;  
42 Tiranti and Deangeli, 2015; Hu et al., 2016). Rainfall is one of the main triggering factors of  
43 debris flows and is the most active factor when debris flows occur, which also determines the  
44 temporal and spatial distribution characteristics of the hazards. As one of the important and  
45 effective means of non-engineering disaster mitigation, much attention has been paid to  
46 debris flow early warning by researchers (Pan et al., 2013; Guo et al., 2013; Zhou et al., 2014;  
47 Wei et al., 2017). For rainstorm triggered debris flows, the precipitation and intensity of rain-  
48 fall are the decisive factors of debris flow initiation, and a reasonable rainfall threshold target  
49 is essential to ensure the accuracy of debris flow early warning. However, if there are some  
50 extreme events occurred, such as an earthquake, the rainfall threshold of debris flow may  
51 change a lot. Tang et al. (2012) analyzed the critical rainfall of Beichuan city and found that  
52 the cumulative rainfall triggering debris flow decreased by 14.8%-22.1% when compared with  
53 the pre-earthquake period, and the critical hour rainfall decreased by 25.4%-31.6%. Chen et al.  
54 (2013) analyzed the pre- and post-earthquake critical rainfall for debris flow of Xiaogangjian  
55 gully and found that the critical rainfall for debris flow in 2011 was approximately 23% lower

56 than the value during the pre-earthquake period. Other researches, such as Chen et al. (2008)  
57 and Shied et al. (2009) has reached similar conclusions that the post-earthquake critical  
58 rainfall for debris flow is markedly lower than that of the pre-earthquake period. The  
59 Guojuanyang gully, a small gully located in the meizoseismal areas of the big earthquake, has  
60 no debris flows under the annual average rainfall before 2008, but it became a debris flow  
61 gully after the earthquake under the same conditions, even the rainfall was smaller than the  
62 annual average rainfall. These indicated that earthquakes have a big influence on debris flow  
63 occurrence. The earthquake triggered many unstable slopes, collapses, and landslides, which  
64 have served as the source material for debris flow and shallow landslide in the years after the  
65 earthquake (Tang et al. 2009, 2012; Xu et al. 2012; Hu et al. 2014). Therefore, the rainfall  
66 threshold of debris flow post-earthquake is an important and urgent issue to study for debris  
67 flow early warning and mitigation.

68 As an important and effective means of disaster mitigation, debris flow early warning  
69 have received much attention from researchers. The rainfall threshold is the core of the debris  
70 flow early warning , on which have a great deal of researches yet (Cannon et al., 2008; Chen  
71 and Huang 2010; Baum and Godt, 2010;Staley et al., 2013; Winter et al., 2013; Zhou and Tang,  
72 2014; Segoni et al., 2015; Rosi et al 2015). Although the formation mechanism of debris flow  
73 has been extensively studied, it is difficult to perform distributed physically based modeling  
74 over large areas, mainly because the spatial variability of geotechnical parameters is very  
75 difficult to assess (Tofani et al., 2017). Therefore, many researchers (Wilson and Joyko, 1997;  
76 Campbell, 1975; Cheng et al., 1998) have had to determine the empirical relationship between  
77 rainfall and debris flow events and to determine the rainfall threshold depending on the  
78 combinations of rainfall parameters, such as antecedent rainfall, rainfall intensity, cumulative  
79 rainfall, et al.. Takahashi (1978), Iverson (1989)and Cui (1991) predicted the formation of  
80 debris flow based on studies of slope stability, hydrodynamic action and the influence of pore  
81 water pressure on the formation process of debris flow. Caine (1980) first statistically  
82 analyzed the empirical relationship between rainfall intensity and the duration of debris flows  
83 and shallow landslides and proposed an exponential expression( $I = 14.82D^{-0.39}$ ). Afterwards,  
84 other researchers, such as Wieczorek (1987), Jison (1989), Hong et al. (2005), Dahal and  
85 Hasegawa (2008), Guzzetti et al. (2008) and Saito et al. (2010), carried out further research

86 on the empirical relationship between rainfall intensity and the duration of debris flows,  
87 established the empirical expression of rainfall intensity - duration ( $I = D$ ) and proposed  
88 debris flow prediction models. Although I-D is the most used approach, other rainfall  
89 parameters have been considered as well for debris flow thresholds. Shied and Chen (1995)  
90 established the critical condition of debris flow based on the relationship between cumulative  
91 rainfall and rainfall intensity. Zhang (2014) developed a model for debris flow forecasting  
92 based on the water-soil coupling mechanism at the watershed scale. In addition, some  
93 researchers have highlighted the importance to find more robust hydrological bases to  
94 empirical rainfall thresholds for landslide initiation (Bogaard et al., 2018; Canli et al., in  
95 review; Segoni et al., 2018). When data are scarce, a robust validation of a threshold model  
96 can be based on a quantitative comparison with alternate versions of the threshold  
97 (Althuwaynee et al., 2015) or with thresholds calculated with completely different approaches  
98 (Frattini et al., 2009; Lagomarsino et al., 2015). Zhenlei Wei et al. (2017) investigated a  
99 rainfall threshold method for predicting the initiation of channelized debris flows in a small  
100 catchment, using field measurements of rainfall and runoff data.

101 Overall, the studies on the rainfall threshold of debris flow can be summarized as two  
102 methods: the demonstration method and the frequency calculated method. The  
103 demonstration method employs statistical analysis of rainfall and debris flow data to study the  
104 relationship between rainfall and debris flow events and to obtain the rainfall threshold curve  
105 (Bai et al., 2008; Tian et al., 2008; Zhuang, et al., 2009). The I-D approaches would be this  
106 kind of method. This method is relatively accurate, but it needs very rich, long-term rainfall  
107 database and disaster information; therefore, it can be applied only to areas with a history of  
108 long-term observations. The frequency calculated method, assuming that debris flow and  
109 torrential rain have the same frequency, and thus, debris flow rainfall threshold can be  
110 calculated based on the rainstorm frequency in the mountain towns where have abundant  
111 rainfall data but lack of disaster data (Yao, 1988; Liang and Yao, 2008). Researchers have also  
112 analyzed the relationship between debris flow occurrences and precipitation and soil moisture  
113 content based on initial debris flow conditions (Hu and Wang, 2003). However, this approach  
114 is rarely applied to the determination of debris flow rainfall thresholds because it needs series  
115 of rainfall data. Pan et al. (2013) calculated the threshold rainfall for debris flow pre-warning

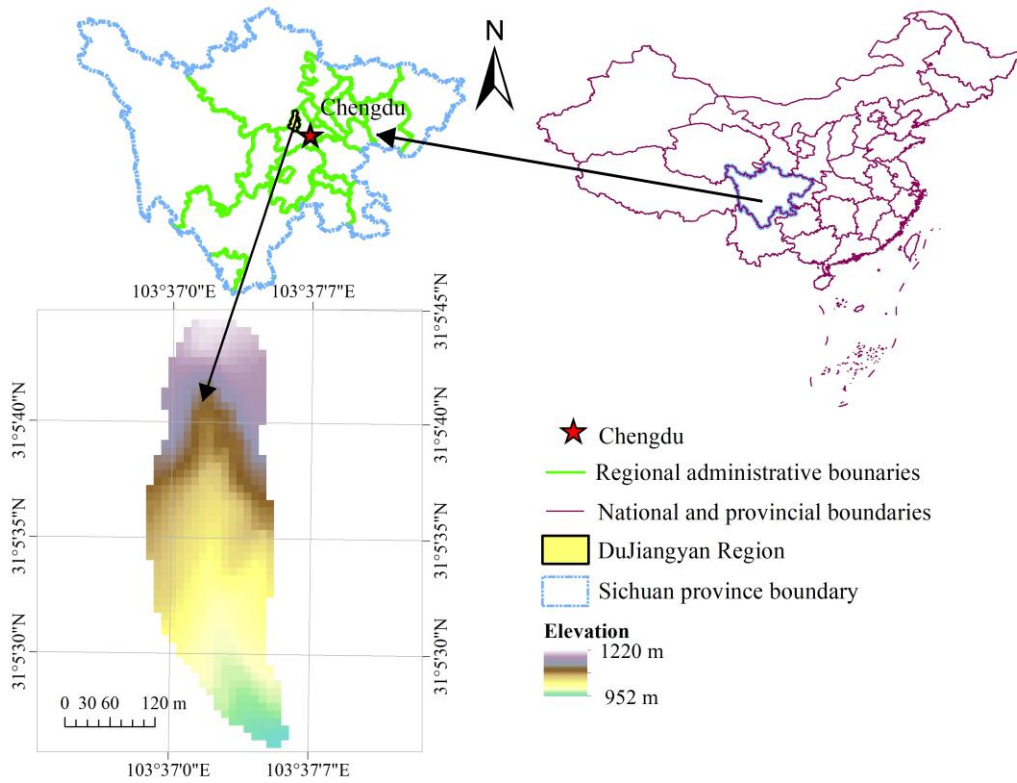
116 by calculating the critical depth of debrisflow initiation combined with the amount and  
117 regulating factors of runoff generation.

118 Most mountainous areas have little data regarding rainfall and hazards, especially in  
119 Western China. Neither the traditional demonstration method nor frequency calculated  
120 method can satisfy the debris flow early warning requirements in these areas. Therefore, how  
121 to calculate the rainfall threshold in these data-poor areas has become one of the most  
122 important challenges for the debris flow early warning systems. To solve this problem, this  
123 paper developed a quantitative method of calculating rainfall threshold for debris flow early  
124 warning in areas with scarcity of data based on the initiation mechanism of hydraulic-driven  
125 debris flows.

## 126 **2 Study site**

### 127 **2.1 Location and gully characteristics of the study area**

128 The Guojuanyan gully in Du Jiangyan city, located in the meizoseismal areas of the  
129 Wenchuan earthquake, China, was selected as the study area (Fig. 1). It is located at the  
130 Baisha River, which is the first tributary of the Minjiang River. The seismic intensity of the  
131 study area was XI, which was the maximum seismic intensity of the Wenchuan earthquake.  
132 The Shenxi Gully Earthquake Site Park is at the right side of this gully. The area extends from  
133  $31^{\circ}05'27''$  N to  $31^{\circ}05'46''$  N latitude and  $103^{\circ}36'58''$  E to  $103^{\circ}37'09''$  E longitude, covering an  
134 area of 0.15 km<sup>2</sup> with a population of 20 inhabitants. The elevation range is from 943 m to  
135 1222 m, the average gradient of the main channel is 270‰ (the average slope angle is 15.1°),  
136 and the length of the main channel is approximately 580m.



137

138

**Figure 1.** The location of the Guojuanyan gully

139

140

141

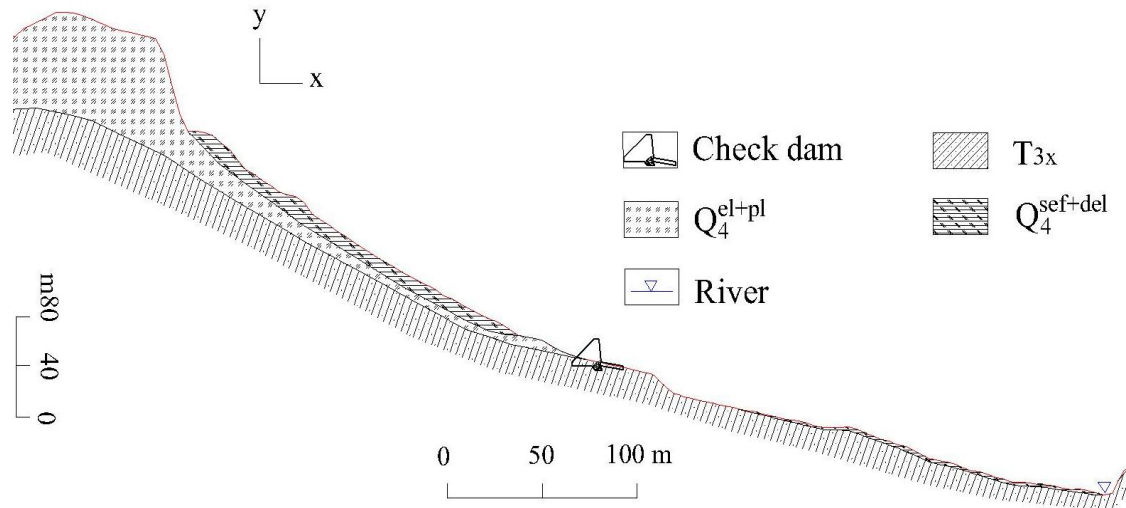
142

143

144

145

Geologically, the Guojuanyan gully is composed of bedrock and Quaternary strata. The bedrock is upper Triassic Xujiahe petrofabric ( $T_3x$ ) whose lithology is mainly sandstone; mudstone; carbonaceous shale belonging to layered, massive structures; and semi solid-solid petrofabric. The Quaternary strata are alluvium ( $Q_4^{el+pl}$ ), alluvial materials ( $Q_4^{pl+dl}$ ), landslide accumulations and debris flow deposits ( $Q_4^{sef+del}$ ). The thickness of the Quaternary strata ranges from 1 m to 20 m and varies greatly. The strata profile of the Guojuanyan gully is shown in Fig. 2.



146

147

**Figure 2.** The strata profile of the Guojuanyan gully (Jun Wang et al, 2017)

148

Geographically, the study area belongs to the Longmenshan Mountains. The famous Longmenshan tectonic belt has a significant effect on this region, especially the Hongkou-Yinxu fault. The study area has strong tectonic movement and strong erosion, and the main channel is “V”-shaped. The area is characterized by a rugged topography, and the main slope gradient interval of the gully is 20° to 40°, accounting for 52.38% of the entire study area.

153

Climatically, this area has a subtropical and humid climate, with an average annual temperature of 15.2°C and an average annual rainfall of 1200 mm (Wang et al., 2014).

154

155

## **2.2 Materials and debris flow characteristics of the study area**

156

The Wenchuan earthquake generated a landslide in the Guojuanyan gully, leading to an abundance of loose deposits that have served as the source materials for debris flows. A comparison of the Guojuanyan gully before and after the Wenchuan earthquake is shown in Fig. 3. According to the field investigation and field tests, the landslide 3D characteristics induced by the earthquake and the infiltration characteristics of the loose materials are shown in Table 1 and Table 2 (Wang et al., 2016). They indicate that the volume of materials is more than  $20 \times 10^4 \text{ m}^3$ , and the infiltration capable of the earth surface have much increased. Therefore, the trigger rainfall for debris flow has decreased greatly. The Guojuanyan gully had no debris flows before the earthquake because of the lack of loose solid materials before the earthquake; however, it became a debris flow gully after the earthquake, and debris flows occurred in the

165

166 following years (Table 3). The specific conditions of these debris flow events were collected  
 167 through field investigations and interviews. The field investigations and experiments deter-  
 168 mined that the density of the debris flow was between 1.8 and 2.1 g/cm<sup>3</sup>. Unfortunately, there  
 169 were no rainfall data before 2011, when we started field surveys in the Guojuanyan gully.



(a) 14 September, 2006 (b) 28 June, 2008

**Figure 3.** The Guojuanyan gully before (a) and after the Wenchuan earthquake (b) (from Google Earth)

**Table 1.** The landslide 3D characteristics induced by the earthquake in the study area

Average length /m	Average width /m	Average Height /m	Average depth /m	Slope /°	Volume /×10 <sup>4</sup> m <sup>3</sup>
160	80	180	15	≅ 30	20

**Table 2.** The infiltration characteristics of solid materials in the study area

Infiltration curve	Infiltration rate	
	Initial infiltration /cm/min	Stable infiltration /cm/min
$f = 0.6529 \cdot \exp(-0.057 \cdot t)$	3.52	0.34

**Table 3.** The specific conditions of debris flow events in the Guojuanyan gully after the earthquake

Time	Volume (10 <sup>4</sup> m <sup>3</sup> )	Surges	Rainfall data record
24 September, 2008	0.6	1	No
17 July, 2009	0.8	1	No
13 August, 2010	4.0	3	No
17 August, 2010	0.4	1	No
1 July, 2011	0.8	1	Yes
17 August, 2012	0.7	1	Yes
9 July, 2013	0.4	1	Yes
26 July, 2013	2.0	2	Yes
18 July, 2014	1.5	1	Yes

177 **2.3 Debris flow monitoring and streambed survey of the study area**

178 After the Wenchuan earthquake, continuous field surveillance was undertaken in the  
179 study area. A debris flow monitoring system was also established in the study area. To identify  
180 the debris flow events, this monitoring system recorded stream water depth, precipitation and  
181 real-time video of the gully (Fig. 4). The water depth was measured using an ultrasonic level  
182 meter, and precipitation was recorded by a self-registering rain gauge. The real-time video  
183 was recorded onto a data logger and transmitted to the monitoring center, located in the In-  
184 stitute of Mountain Hazards and Environment, Chinese Academy of Sciences. When a rain-  
185 storm or a debris flow event occurs, the realtime data, including rainfall data, video record,  
186 and water depth data, can be observed and queried directly in the remote client computer in  
187 the monitoring center. Fig. 5 shows images taken from the recorded video. These data can be  
188 used to analyze the rainfall or other characteristics, such as the 10-min, 1- and 24-h critical  
189 rainfall. The recorded video is usually used to analyse the whole inundated process of debris  
190 flow events and to identify debris flow events as well as the data from rainfall, flow depth, and  
191 field investigation.



192 (a) Real-time camera and rain gauge (b) Ultrasonic level meters

193 **Figure 4.** Debris flow monitoring system in the study area

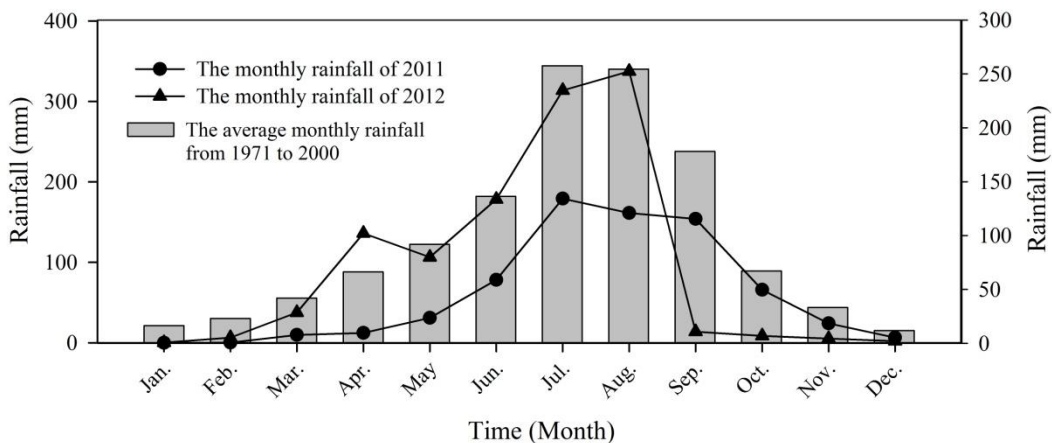


195

197 **2.4 Data collection and the characteristics of rainfall**

198 The Wenchuan earthquake occurred in the Longmenshan tectonic belt, located on the  
 199 eastern edge of the Tibetan plateau, China, which is one of three rainstorm areas of Sichuan  
 200 Province (Longmen mountain rainstorm area, Qingyi river rainstorm area and Daba moun-  
 201 tain rainstorm area). Heavy rainstorms and extreme rainfall events occur frequently. Because  
 202 there were few data in the mountain areas, we collected the rainfall data from 1971- 2000 and  
 203 2011-2012 (from our own on-site monitoring); the characteristics of the rainfalls are as fol-  
 204 lowing:

205 (1) Abundant precipitation: The average annual precipitation was 1177.3 mm from 1971 to  
 206 2000, and the average monthly precipitation is shown in Fig. 6. From 1971 to 2000, the min-  
 207 imum annual precipitation of 713.5 mm occurred in 1974, and the maximum annual precipi-  
 208 tation of 1605.4 mm occurred in 1978. The total precipitation in 2012 is 1148mm, in the trend  
 209 range of the historical data.



210

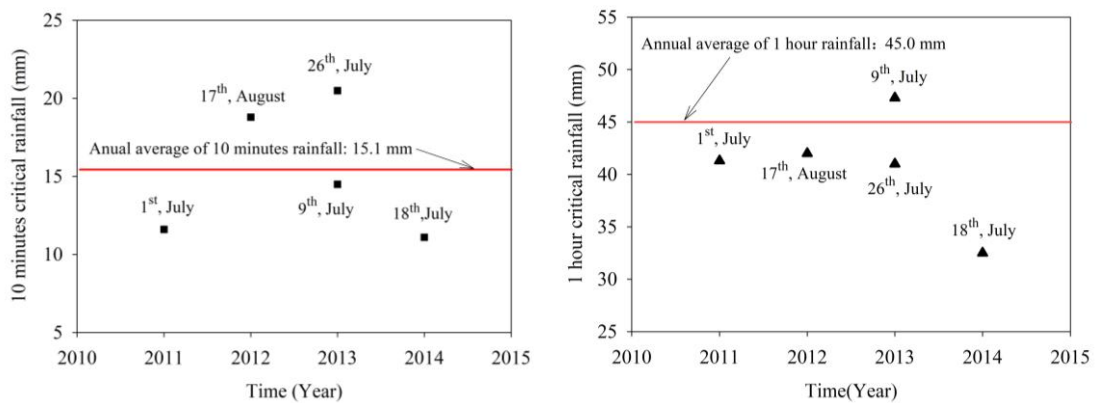
211 **Figure 6.** The average monthly precipitation of the Guojuanyan gully from 1971 to 2000 and the  
 212 monthly rainfall of 2011 and 2012

213 (2) **Seasonality of the distribution of precipitation:** from Fig. 6 we can observe that rain-  
 214 fall is seasonal, with approximately 80% of the total rainfall occurring during the monsoon  
 215 season (from June to September) and the other 20% in other seasons. And the laws of  
 216 monthly rainfall in 2011 and 2012 coincide to the historical data. For instance, in 2012, the

217 total annual rainfall in this area was approximately 1148 mm, and rainfall in the monsoon  
 218 season from June to September was 961 mm, accounting for 83.7% of the annual total.

219 (3) The rainfall intensity has great differences. From 1971 to 2000, the maximum month-  
 220 ly rainfall was 592.9 mm, the daily maximum rainfall was 233.8 mm, the hourly maximum  
 221 rainfall was 83.9 mm, the 10 minute maximum rainfall was 28.3 mm, and the longest contin-  
 222 uous rainfall time was 28 days.

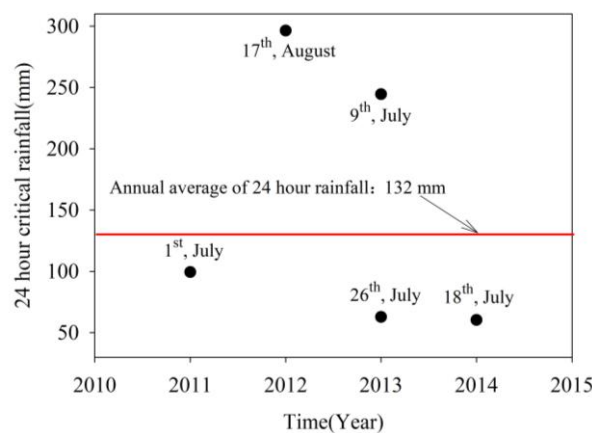
223 Debris flow field monitoring data and on-site investigation data were used to identify the  
 224 debris flow events and to analyze the characteristics of the rainfall pattern and the critical  
 225 rainfall characteristics. Analyzing the typical rainfall process curves (Fig. 13), we can find that  
 226 the hourly rainfall pattern of the Guojuanyang gully is the peak pattern, displaying the single  
 227 peak and multi-peak, a characteristic of short-duration rainstorms. Through the statistical  
 228 analysis of the 10-min, 1-, and 24-h critical rainfall of debris flow events after the earthquake,  
 229 their characteristics can be obtained, as shown in Fig. 7.



230

231

(a) The 10-min critical rainfall (b) The 1-h critical rainfall



232

233

(c) The 24-h critical rainfall

234

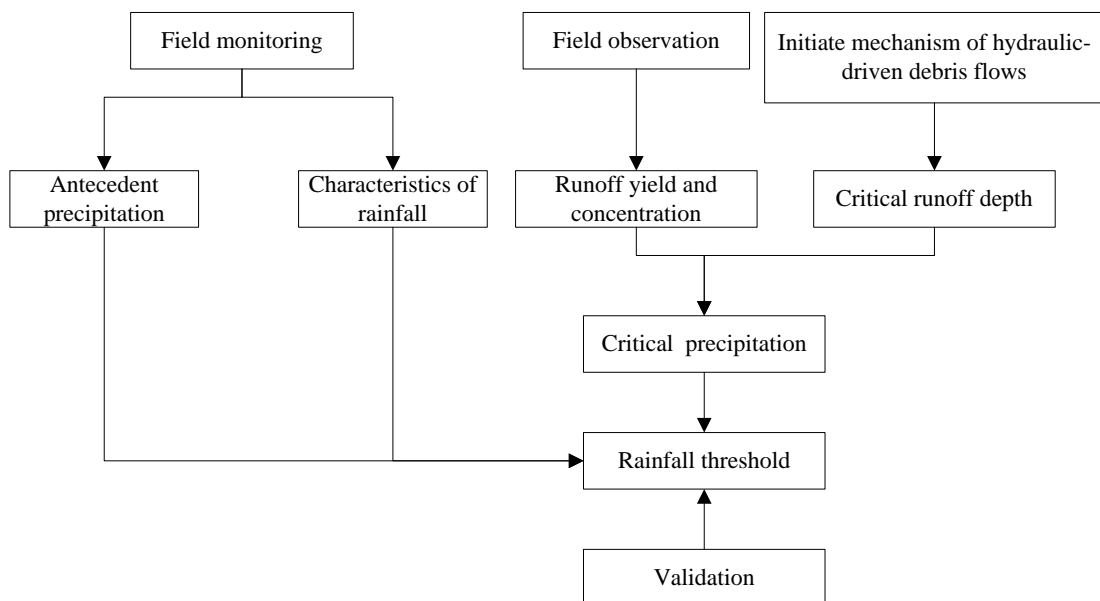
**Figure 7.** The critical rainfall of debris flows in the Guojuanyan gully

235 According to the Sichuan Hydrology Record Handbook (Sichuan Water and Power De-  
 236 partment 1984), during 1940-1975, the annual average of maximum 10-min rainfall of the  
 237 study area is approximately 15.1 mm, the maximum 1-h rainfall is 45.0 mm and the annual  
 238 average of maximum 24-h rainfall is 132 mm. Fig. 7 shows that the majority of the debris flow  
 239 events in 2011-2014 occurred in a rainfall below the annual average values. It convinced that  
 240 the rainfall threshold of debris flow was decreased obviously after the earthquake.

### 241 3 Materials and methods

242 This study makes an attempt to analyze the trigger rainfall threshold for debris flow by  
 243 using the initiation mechanism of debris flow. Firstly, to analyze the rainfall characteristics of  
 244 the watershed by using the field monitoring data; then to calculate the runoff yield and con-  
 245 centration progress based on field observation. Additionally, the critical runoff depth to initi-  
 246 ate debris flow was calculated by the initiation mechanism with the underlying surface condi-  
 247 tion (materials, longitudinal slope, etc.) of the gully. Then, the corresponding rainfall for the  
 248 initiation of debris was back-calculated based on the stored- full runoff generation. At last,  
 249 these factors were combined to build the rainfall threshold model. This method can be applied  
 250 to the early warning system in the areas with scarcity of rainfall data.

251 The flow chart of the research is shown in Fig. 8.



252  
 253

254

**Figure 8.** The flow chart of the research

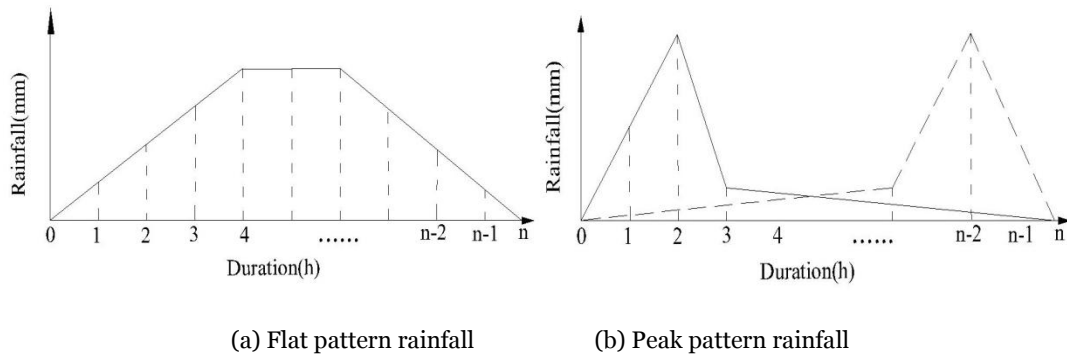
255 The main influence factors for the formation of debris flow event include three parts: a  
256 steep slope of the gully (served as potential energy condition), abundant solid materials  
257 (source condition) and water source condition (usually is rainfall condition for rainstorm  
258 debris flow). For rainstorm debris flow events, the precipitation and intensity of rainfall are  
259 the decisive factors of debris flow initiation. If there is no earthquakes or other extreme events,  
260 the topography of the gully can be considered relatively stable. In contrast, rainfall conditions  
261 and the distribution of solid materials that determine the occurrence of debris flows can  
262 display temporal and spatial variation within the same watershed. Therefore, it is common to  
263 provide warning of debris flows based rainfall data after assessing the supply and distribution  
264 of loose solid materials. In Takahashi's model, the characteristics of soil, such as the porosity  
265 and the hydraulic conductivity of soils, are not considered, and considered the characteristic  
266 particle size and the volume concentration of sediment; while the characteristics of  
267 topography is mainly represented by the longitudinal slope of the gully. Furthermore, in the  
268 stored-full runoff model, the maximum storage capacity of watershed, which mainly decided  
269 by the porosity and permeability of the soil, may represent the characteristic of the hydraulic  
270 conductivity of solid material to a certain extent. Therefore, this study wouldn't consider the  
271 hydraulic conductivity any more.

### 272 **3.1 Rainfall pattern and the spatial-temporal distribution characteristics**

273 Mountain hazards such as debris flows are closely related to rainfall duration, rainfall  
274 amount and rainfall pattern (Liu et al., 2009). Rainfall pattern not only affects the formation  
275 of surface runoff but also affects the formation and development of debris flows. Different  
276 rainfall patterns result in different soil water contents; thus, the internal structure of the soil,  
277 stress conditions, shear resistance, slip resistance and removable thickness can vary. The ini-  
278 tiation of a debris flow is the result of both short-duration heavy rains and the antecedent  
279 rainfall (Cui et al., 2007; Guo et al., 2013). Many previous observational data have shown that  
280 the initiation of a debris flow often appears at a certain time that has a high correlation with  
281 the rainfall pattern (Rianna et al., 2014; Mohamad Ayob Mohamadi, 2015).

282 The precipitation characteristics not only affect the formation of runoff, also affect the  
283 formation and development of the debris flow. Different rainfalls result in different soil water  
284 contents, and thus the internal structure of the soil, stress conditions, corrosion resistance

285 and slip resistance can vary (Pan et al., 2013). Based on the rainfall characteristics, rainfall  
 286 patterns can be roughly divided into two kinds, the flat pattern and the peak pattern, as shown  
 287 in Fig. 9. If the rainfall intensity has little variation, there is no obvious peak in the whole  
 288 rainfall process; such rainfall can be described as flat pattern rainfall. **If the soils characterized**  
 289 **by low hydraulic conductivity, this kind of rainfall can hardly trigger a debris flow separately,**  
 290 **and the debris flows will mainly be triggered by the great amount of effective antecedent pre-**  
 291 **precipitation.** While if the rainfall intensity increases suddenly during a certain period of time,  
 292 the rainfall process will have an obvious peak and is termed peak pattern rainfall. If the hy-  
 293 draulic conductivity is high enough, the rainfall can totally entering the soil and mass can  
 294 move easily. These debris flows are mainly controlled by the short-duration heavy rains. Peak  
 295 pattern rainfall may have one peak or multi-peak (Pan, et al., 2013).



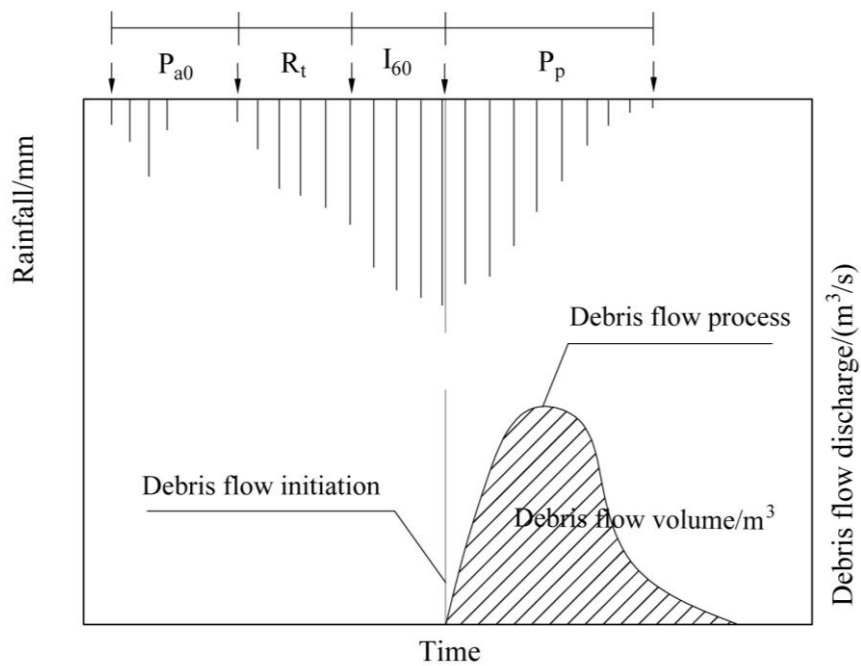
298 **Figure 9.** The diagram of rainfall patterns

299 Through analyzing the rainfall data of the Guojuanyan gully, the rainfall pattern and the  
 300 spatial-temporal distribution characteristics can be obtained.

301 **3.2 The calculation of the antecedent precipitation index ( API )**

302 The rainfall factor influencing debris flows consists of three parts: indirect antecedent  
 303 precipitation (IAP) (it is  $P_{a0}$  in this paper), direct antecedent precipitation (DAP) (it is  $R_t$  in this  
 304 paper), and triggering precipitation (TP) (it is  $I_{60}$  in this paper). The relationships among them  
 305 are shown in Figure 10. Obviously, IAP increases soil moisture and decreases the soil stability,  
 306 and DAP saturates soils and thus decrease the critical condition of debris flow occurrence.  
 307 Although TP is believed to initiate debris flows directly, its contribution amounts to only 37%  
 308 of total water (Cui et al. 2007). Guo et al (2013) analyzed the rainstorms and debris flow

309 events during June and September in 2006 and 2008, there were 208 days with antecedent  
 310 rainfall more than 10mm, approximately 57% days of the rain season. Among them, there  
 311 were 66 days with antecedent rainfall between 10-15mm, and 1 debris flow event happened;  
 312 53 days between 15-20 mm and 4 debris flow events happened; 28 days between 20-25 mm  
 313 and 4 debris flow events happened; 30 days between 25-33 mm and 5 debris flow happened;  
 314 and 35 days more than 33mm and 9 debris flow events happened. So this group of data can  
 315 specifically illustrate the importance of the antecedent rainfall to the debris flow events.



316

317 **Figure 10. Rainfall index classifications**

318 As Fig. 10 shows, take 1-h rainfall ( $I_{60}$ ) that obtained from the observed data of the  
 319 Guojuanyan gully for the TP. The antecedent precipitation index ( $API$ ) includes IAP and  
 320 DAP, calculated as the following expression (Zhao, 2011; Guo, 2013; Zhuang, 2015):

321 
$$API = P_{a0} + R_t \quad (1)$$

322 where  $P_{a0}$  is the effective antecedent precipitation (mm) and  $R_t$  is the direct antecedent precip-  
 323 itation (mm), which is the precipitation from the beginning of the rainfall that trigger debris  
 324 flow to the 1 hour before the debris flow.

325 It's difficult to study the influence of antecedent rainfall to debris flow as it mainly relies  
 326 on the heterogeneity of soils (strength and permeability properties), which makes it hard to  
 327 measure the moisture. Usually, the frequently used method for calculating antecedent daily  
 328 rainfall is the weighted sum equation as below (Crozier and Eyles 1980; Glade et al. 2000):

329

$$P_{a0} = \sum_1^n P_i \cdot K_i \quad (2)$$

330

Where  $P_i$  is the daily precipitation in the  $i$ -th day proceeding to the debris flow event

331

( $1 \leq i \leq n$ ) and  $K_i$  is a decay coefficient due to evaporation and geomorphological conditions

332

of the soil. The value of the  $K$ , is typically 0.8-0.9, can be determined by the test of soil mois-

333

ture content based on Eq.2 in the watershed. The effect of a rainfall event usually diminishes

334

with the time going forward. Different patterns of storm debris flow gullies require different

335

numbers of previous indirect rainfall days ( $n$ ), which can be determined by the relationship

336

between the triggering rainfall and the antecedent rainfall of a debris flow (Pan, et al., 2013).

337

If the rainfall is sharp and heavy, the initiation of debris flow would mainly be determined by

338

DAP and TP, while the influence of the antecedent precipitation would be decreased, and vice

339

versa.

340

### 3.3 The rainfall threshold curve of debris flows

341

#### 3.3.1 The initiation mechanism of hydraulic-driven debris flows

342

When the watershed hydrodynamics, which include the runoff, soil moisture content and

343

the discharge, reach to a certain level, the loose deposits in the channel bed will initiate

344

movement and the sediment concentration of the flow will increase, leading the sediment

345

laden flow to transform into a debris flow. The formation of this kind of debris flow is a com-

346

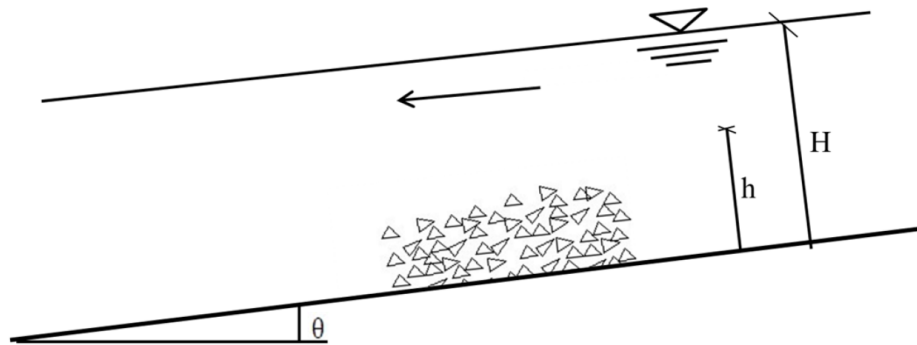
pletely hydrodynamic process. Therefore, it can be regarded as the initiation problem of de-

347

bris flow under hydrodynamic force. The forming process of hydraulic-driven debris flows is

348

shown in Fig. 10.



349

350

Figure 11. The typical debris flow initiate model

351 According to Takahashi's model, the critical depth for hydraulic-driven debris flows is:

$$352 \quad h_0 = \left[ \frac{C_*(\sigma - \rho) \tan \phi}{\rho \tan \theta} - \frac{C_*(\sigma - \rho)}{\rho} - 1 \right] d_m \quad (3)$$

353 where  $C_*$  is the volume concentration obtained by experiments(0.812);  $\sigma$  is the unit weight of  
354 loose deposits (usually is 2.65 g/cm<sup>3</sup>);  $\rho$  is the unit weight of water,1.0 g/cm<sup>3</sup>;  $\theta$  is the chan-  
355 nel bed slope (°);  $\phi$  is the internal friction angle (°) and can be measured by shear tests ;

356 And  $d_m$  is the average grain diameter (mm), which can be expressed as:

$$357 \quad d_m = \frac{d_{16} + d_{50} + d_{84}}{3} \quad (4)$$

358 where  $d_{16}$ ,  $d_{50}$  and  $d_{84}$  are characteristic particle sizes of the loose deposits (mm), whose  
359 weight percentage are 16%, 50% and 84% separately.

360 Takahashi's model became one of the most common for the initiation of debris flow after  
361 it was presented. A great deal of related studies was published based on Takahashi's model  
362 later. **Some discussed the laws of debris flow according to the geomorphology and the water**  
363 **content (Sassa et al., 2010; Wang, 2016), while others examined the critical conditions of de-**  
364 **bris flow with mechanical stability analysis (Cao et al., 2004; Jiang et al., 2017).** However,  
365 Takahashi's relation was determined for debris flow propagating over a rigid bed, hence, with  
366 a minor effect of quasi-static actions near the bed. Lanzoni et al. (2017) slightly modified the  
367 Takahashi's formulation of the bulk concentration, which considered the long lasting grain  
368 interactions at the boundary between the upper, grain inertial layer and the underlying static  
369 sediment bed, and validated the proposed formulation with a wide set of experimental data  
370 (Takahashi, 1978, Tsubaki et al., 1983, Lanzoni, 1993, Armanini et al., 2005). The effects of  
371 flow rheology on the basis of velocity profiles are analyzed with attention to the role of differ-  
372 ent stress-generating mechanisms.

373 This study aims to the initiation of loose solid materials in the gully under surface runoff;  
374 the interactions on the boundary are not involved. Therefore, Takahashi's model can be used  
375 in this study.

### 376 **3.3.2 Calculation of watershed runoff yield and concentration**

377 **The stored-full runoff, one of the modes of runoff production, is also called as the super**

378 storage runoff. The reason of the runoff yeild is that the aeration zone and the saturation zone  
 379 of the soil are both saturated. In the humid and semi humid areas where rainfall is plentiful,  
 380 because of the high groundwater level and soil moisture content, when the losses of precipita-  
 381 tion meet the plant interception and infiltration, it would not increase anymore with the rains  
 382 continuous. The Guojuanyan gully is located in Du Jiangyan city, which is in a humid area.  
 383 Therefore, stored-full runoff can be used to calculate the watershed runoff. That is, it can be  
 384 supposed that the water storage can reach the maximum storage capacity of the watershed in  
 385 each heavy rain event. Therefore, the rainfall loss in each time  $I$  is the difference between the  
 386 maximum water storage capacity  $I_m$  and the soil moisture content before the rain  $P_a$ . The wa-  
 387 ter balance equation of stored-full runoff is expressed as follows (Ye, et al., 1992):

$$388 \quad R = P - I = P - (I_m - P_a) \quad (5)$$

389 where  $R$  is the runoff depth (mm);  $P$  is the precipitation of one rainfall (mm);  $I$  is the rain-  
 390 fall loss (mm);  $I_m$  is the watershed maximum storage capacity (mm) for a certain watershed,  
 391 it is a constant for a certain watershed that can be calculated by the infiltration curve or infil-  
 392 tration experiment data. In this study,  $I_m$  has been picked up from Handbook of rainstorm  
 393 and flood in Sichuan (Sichuan Water and Power Department 1984); and  $P_a$  is the antecedent  
 394 precipitation index, referring to the total rainfall prior to the 1 hour peak rainfall leading to  
 395 debris flow initiation.

396 Eq. 5 can be expressed as follows:

$$397 \quad P + P_a = R + I_m \quad (6)$$

398 The precipitation intensity is a measure of the peak precipitation. At the same time, the  
 399 duration of the peak precipitation is generally brief, lasting only up to tens of minutes. There-  
 400 fore, 10-minute precipitation intensity (maximum precipitation over a 10-minute period dur-  
 401 ing the rainfall event) is selected as the triggering rainfall for debris flow, which is appropriate  
 402 and most representative. However, it is difficult to obtain such short-duration rainfall data in  
 403 areas with scarcity of data. Therefore, in this study,  $P$  and  $P_a$  are replaced by  $I_{60}$  (1 hour  
 404 rainfall) and  $API$  (the antecedent precipitation index), respectively; thus, Eq. 6 is expressed  
 405 as:

$$406 \quad I_{60} + API = R + I_m \quad (7)$$

407 In the hydrological study, the runoff depth  $R$  is:

$$408 \quad R = \frac{W}{1000F} = \frac{3.6 \sum Q \cdot \Delta t}{F} = \frac{3.6Q}{F} \quad (8)$$

409 where  $R$  is the runoff depth (m);  $W$  is the total volume of runoff (m<sup>3</sup>);  $F$  is the watershed area  
410 (km<sup>2</sup>);  $\Delta t$  is the duration time, in this study it is 1 hour; and  $Q$  is the average flow of the water-  
411 shed (m<sup>3</sup>/s), which can be expressed as follows:

$$412 \quad Q = BVh_0 \quad (9)$$

413 where  $B$  is the width of the channel (m),  $V$  is the average velocity (m/s) and  $h_0$  is the critical  
414 depth (m).

415 Eq. 7 is the expression of the rainfall threshold curve for a watershed, which can be used  
416 for debris flow early warning. This proposed rainfall threshold curve is a function of the ante-  
417 cedent precipitation index ( $API$ ) and 1 hour rainfall ( $I_{60}$ ), which is a line and a negative  
418 slope.

## 419 **4 Results**

### 420 **4.1 The rainfall threshold curve of debris flow**

#### 421 **4.1.1 The critical depth of the Guojuanyan gully**

422 The grain grading graph (Fig. 11) is obtained by laboratory grain size analysis experi-  
423 ments for the loose deposits of the Guojuanyan gully. Figure 11 shows that the characteristic  
424 particle sizes  $d_{16}$ ,  $d_{50}$ ,  $d_{84}$  and  $d_m$  are 0.18 mm, 1.9 mm, and 10.2 mm, 4.1 mm, respective-  
425 ly. According to Eq. (1), the critical depth ( $h_0$ ) of the Guojuanyan gully is 7.04 mm.

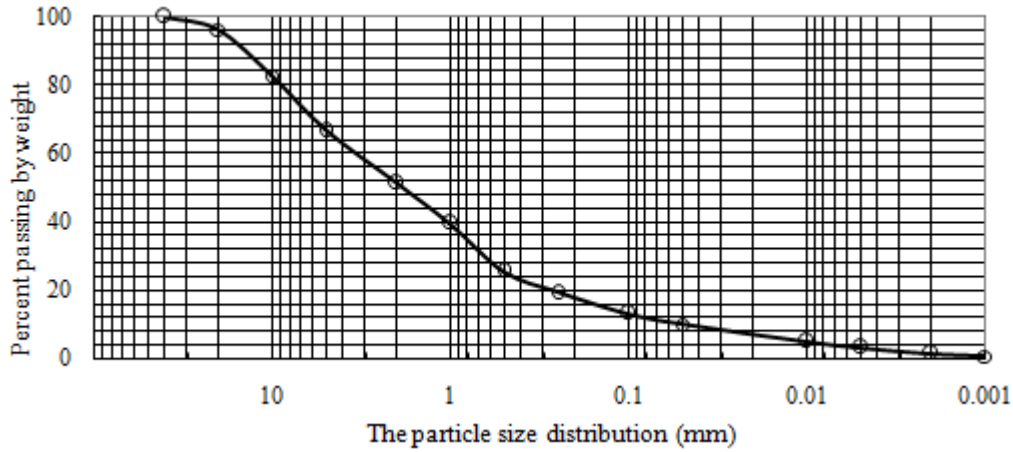


Figure 11. The grain grading graph of the Guojuanyan gully

426  
427

428 **Table 4.** Critical water depth of debris flow triggering in Guojuanyan gully

$C_*$	$\sigma$ (g/cm <sup>3</sup> )	$\rho$ (g/cm <sup>3</sup> )	$\tan \theta$	$d_{16}$ (mm)	$d_{50}$ (mm)	$d_{84}$ (mm)	$d_m$ (mm)	$\phi$ (°)	$\tan \phi$	$h_0$ (mm)
0.812	2.67	1.0	0.333	0.18	1.9	10.2	4.1	21.21	0.388	7.04

#### 429 4.1.2 The rainfall threshold curve of debris flow

430 Taking the cross-section at the outlet of the debris flow formation region as the computa-  
 431 tion object, based on the field investigations and measurements, the width of the cross-section  
 432 is 20 m, and the average velocity of debris flows which is calculated by the several debris flow  
 433 events, is 1.5m/s. Based on the Handbook of rainstorm and flood in Sichuan (Sichuan Water  
 434 and Power Department 1984), the watershed maximum storage capacity ( $I_m$ ) of the  
 435 Guojuanyan gully is 100mm. According to Eq. (5) - Eq. (7), the calculated rainfall threshold  
 436 curve of debris flow in the Guojuanyan gully is shown in Table 5.

437 **Table 5.** The calculated process of the rainfall threshold

Watershed	$h_0$ (mm)	$B$ (m)	$V$ (m/s)	$Q$ (m <sup>3</sup> /s)	$\Delta t$ (h)	$F$ (km <sup>2</sup> )	$R$ (mm)	$I_m$ (mm)	$R + I_m$ (mm)
Guojuanyan	7.04	20.0	1.5	0.197	1	0.11	6.9	100	106.9

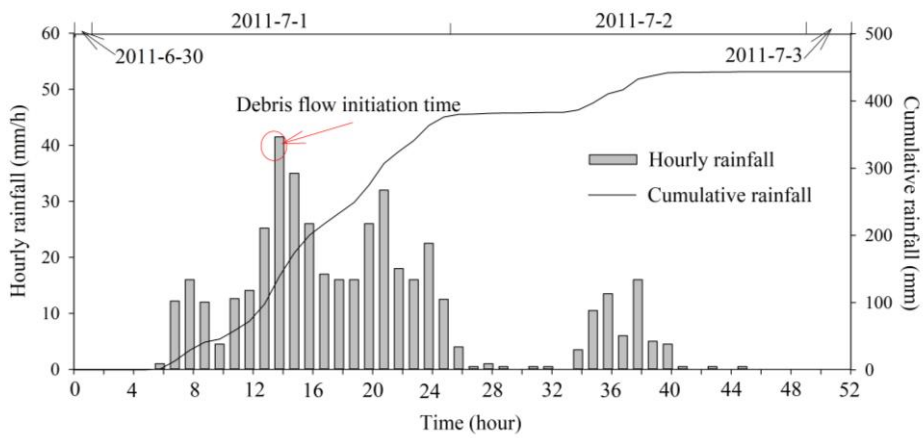
438 From the calculated results, we can conclude the rainfall threshold of the debris flow is  
 439  $I_{60} + API = R + I_m = 106.9 \approx 107$  mm; that is, when the sum of the antecedent precipitation in-  
 440 dex ( $API$ ) and the 1 hour rainfall ( $I_{60}$ ) reaches 107 mm (early warning area), the gully may

441 trigger debris flow.

## 442 4.2 Validation of the results

### 443 4.2.1 The typical debris flow events in the Guojuanyan gully after earthquake

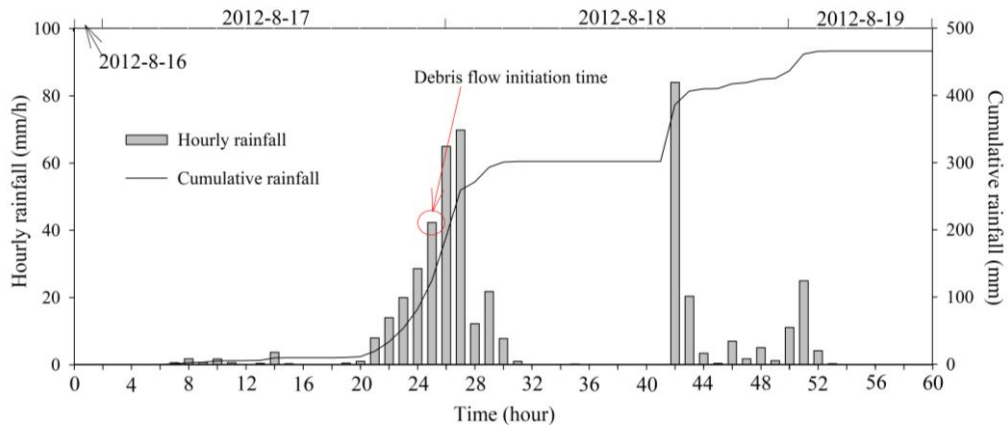
444 Five typical debris flow events and the corresponding rainfall processes are showed in  
445 Figure 13. The debris flow initiation time and the rainfall, both hourly rainfall and cumulative  
446 rainfall, have been recorded. From Fig.13, the five debris flows were triggered by torrential  
447 rains.



448

(a)

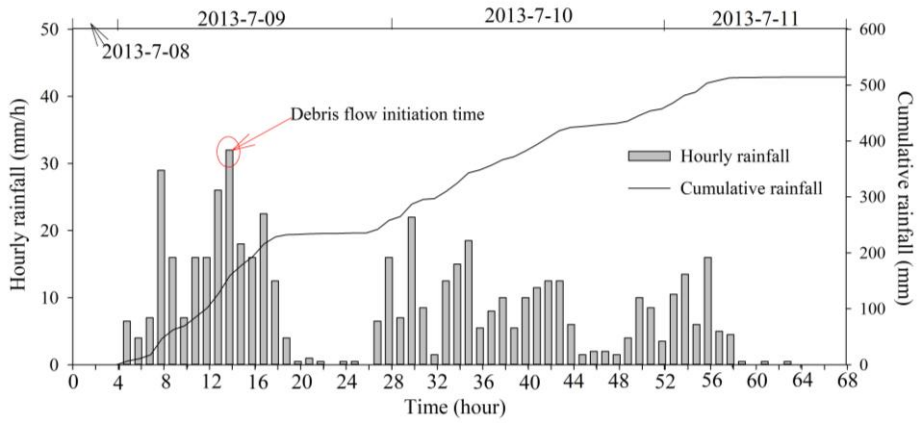
449



450

(b)

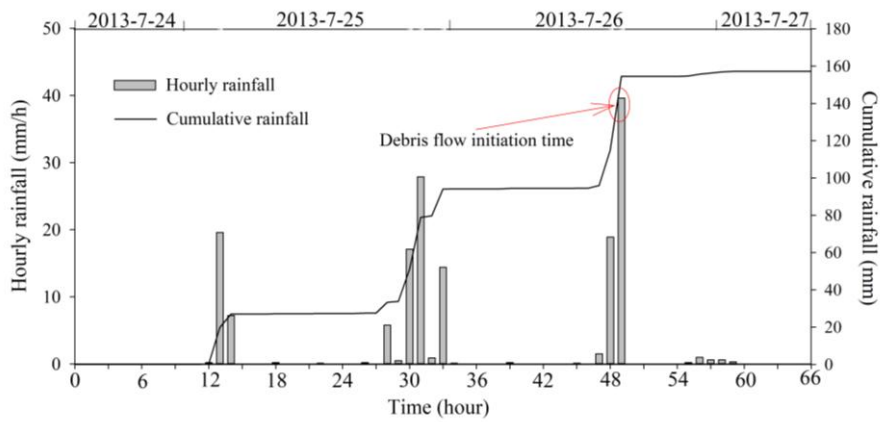
451



452

453

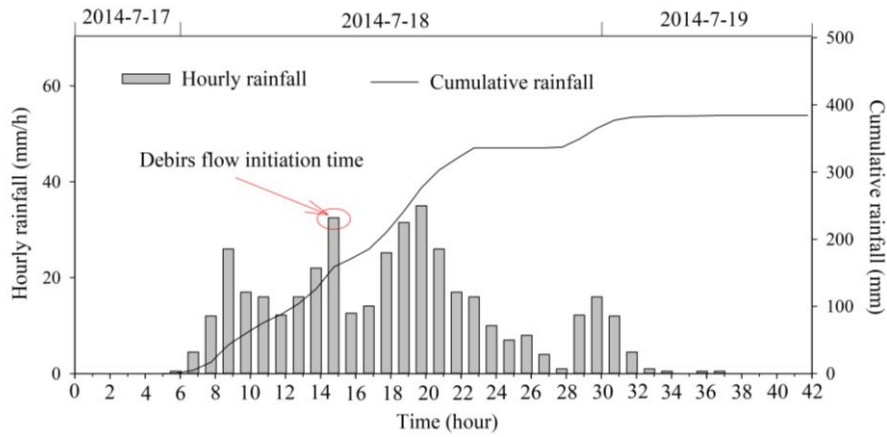
(c)



454

455

(d)



456

457

(e)

458 **Figure 13.** The rainfall process of debris flow events in the Guojuanyan gully from 2011 to 2014 (a, July  
 459 1, 2011; b, August 17, 2012; c, July 9, 2013; d, July 26, 2013; e, July 18, 2014)

460 **4.2.2 The calculation of API and 1-h triggering rainfall of the typical rain-**  
 461 **storms during 2010-2014**

462 Based on the field tests and experiences, the value of  $K$  in Eq.2 is identified as 0.8 (Cui et  
463 al. 2007). To determine the numbers of previous indirect rainfall days ( $n$ ), a comparison  
464 among 3 days, 10days, 20days and 30 days were showed in Table 6. It indicates that the val-  
465 ue of the effective antecedent precipitations ( $P_{a0}$ ) were increasing from 3 days to 20 days,  
466 while with the time last to 30 days, the value of  $P_{a0}$  was barely changed. Therefore, it can be  
467 considered that the effect of a rainfall event usually diminished in 20 days. Hence, the num-  
468 bers of previous indirect rainfall days ( $n$ ) is identified as 20.

469 **Table 6.** The comparisons of  $P_{a0}$  when  $n$  have different values

Time	$P_{a0}(\text{mm})$			
	n=3	n=10	n=20	n=30
July 1, 2011	3.4	5.2	9.7	9.7
August 17, 2012	2.3	4.7	12.1	12.1
July 9, 2013	0.8	2.5	5.7	5.7
July 26, 2013	6.2	10.8	22.4	22.6
July 18, 2014	0	6.2	10.7	10.7
August 20, 2011	8.3	0	8.5	8.6
September 5, 2011	21.3	45.9	48.7	48.8
June 16, 2012	0	2.7	5.6	5.6
August 3, 2012	5.6	6.1	7.5	7.5
August 18, 2012	10.2	18.4	54.3	54.3
June 18, 2013	0	2.8	6.2	6.2
July 28, 2013	0.2	1.7	13.4	13.5
August 6, 2013	0.2	6.6	12.4	12.4

470

471 Thus, the intensity of the 1-h triggering rainfall  $I_{60}$  and cumulative rainfall for the typi-  
472 cal rainstorms are shown in Table 7. In addition to the rainfall process of the 5 debris flow  
473 events (Fig. 13), some typical rainfalls whose daily rainfall were greater than 50 mm but did  
474 not trigger a debris flow were also calculated as a contrast; the greatest 1-h rainfall is consid-  
475 ered as  $I_{60}$ .

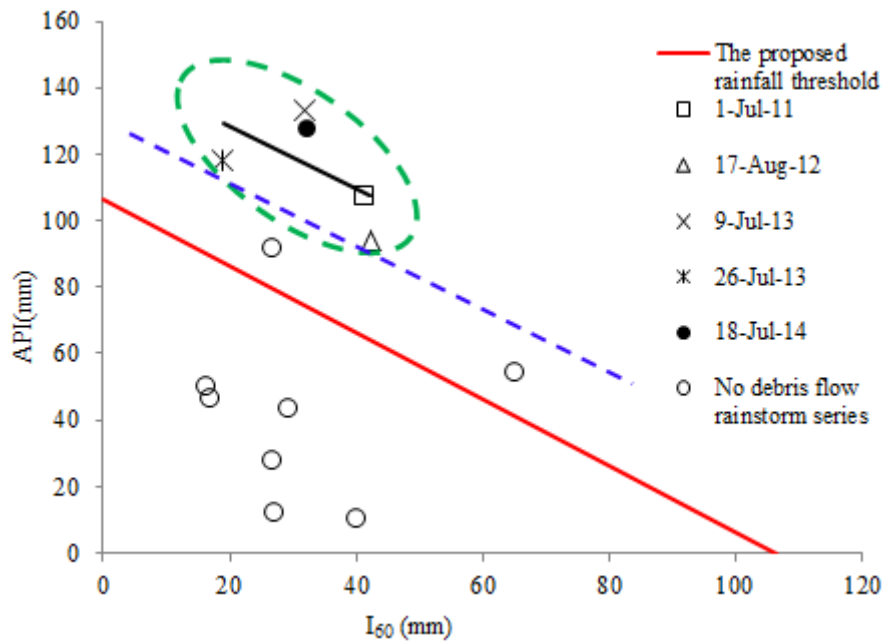
476 **Table 7.** The data of typical rainfall in the Guojuanyan gully after the earthquake

Time	Daily rainfall (mm)	$P_{a0}$ (mm)	$R_t$ (mm)	$API$ (mm)	$I_{60}$ (mm)	$API+I_{60}$ (mm)	Location to the threshold line	Triggered debris flow
1 July, 2011		9.7	97.6	107.3	41.5	148.8	Above	Yes
17 August , 2012		12.1	81.9	94.0	42.3	136.3	Above	Yes
9 July , 2013		5.7	127.5	133.2	32	165.2	Above	Yes
26 July , 2013		22.4	96.0	118.4	18.9	137.3	Above	Yes
18 July, 2014		10.7	116.2	126.9	32.5	159.4	Above	Yes
20 August , 2011	82.8	8.5	19.0	27.5	26.8	54.3	Below	No
5 September , 2011	52.1	48.7	1.2	49.9	16.2	66.1	Below	No

16 June , 2012	55.8	5.6	6.6	12.2	27.0	39.2	Below	No
3 August , 2012	148.3	7.5	84.3	91.8	26.7	118.5	Above	No
18 August , 2012	125.7	54.3	0	54.3	65.0	119.3	Above	No
18 June , 2013	50.6	6.2	3.8	10.0	40.0	50.0	Below	No
28 July , 2013	59.4	13.4	30.0	43.4	29.4	72.8	Below	No
6 August , 2013	56.1	12.4	34.0	46.4	17.1	63.5	Below	No

477

478 The proposed rainfall threshold curve is shown in Figure 14, in which the red real line de-  
479 fines the threshold relationship. It shows that the calculated values  $I_{60} + API$  of debris flow  
480 events in the Guojuanyan gully are all above the rainfall threshold curve, while most of the  
481 rainstorms that did not trigger debris flow are lay below the curve. Therefore, it indicates that  
482 the rainfall threshold curve calculated by this work is reasonable through the validation by  
483 rainfall and hazards data of the Guojuanyan gully.



484

485 **Figure 14.** The calculated rainfall threshold curve (red real line), the trend line (black real line) of the  
486 debris flow events and the debris flows triggering thresholds (dashed line) in Guojuanyan gully

## 487 5 Discussions

488 The trend of the debris flow events as well as the debris flow thresholds were analyzed in  
489 Fig. 14 by using the monitoring rainfall data. A comparison between the thresholds and the  
490 calculated threshold curve indicates that they have the same laws. Therefore, the threshold  
491 calculated method proposed in this work is reasonable and can be used in the areas with scar-  
492 city of data. The proposed rainfall threshold curve is a function of the antecedent precipita-

493 tion index ( $API$ ) and the 1-h rainfall ( $I_{60}$ ), which has been validated by rainfall and hazards  
494 data. It should be noted that the proposed approach is based on a procedure that can be ex-  
495 ported elsewhere only if a site-specific calibration is needed to develop specific thresholds for  
496 other test sites. Therefore, the specific value of the threshold should be calculated by the initi-  
497 ation conditions of the debris flow in specific gully.

498 However, this work still has two limitations. In Figure 14, there are two points above the  
499 curve that did not trigger debris flow at all. Although we have highlighted the significance and  
500 interconnect of antecedent rainfall, critical rainfall, 1-h triggering rainfall, as well as their ac-  
501 curate determination before the hour of debris flow triggering, it should be noticed that the  
502 rainfall is only the triggering factor of debris flows. A comprehensive warning system must  
503 contain more environmental factors, such as the geologic and geomorphologic factors, the  
504 distribution of material source. In addition, the special and complex formative environment of  
505 debris flow after earthquake caused the rainfall threshold is much more complex and uncer-  
506 tain. The rainfall threshold of debris flow is influenced by the antecedent precipitation index  
507 ( $API$ ), rainfall characteristics, amount of loose deposits, channel and slope characteristics,  
508 and so on. Therefore, we should further study the characteristics of the movable solid materi-  
509 als, the shape of gully, and so on to modify the rainfall threshold curve. But, on the other  
510 hand, if given the two rainstorms under the threshold, all the debris flow events points will  
511 still locate above the threshold and there will have no missed alarms. Therefore, the threshold  
512 established in this work is a conservative one and respect safety.

513 On the other hand, restricted by the limited rainfall data, this study was validated by only  
514 5 debris flow events. Another limitation of this work is that the approach proposed in this  
515 study hasn't been validated by other gullies except the Guojuanyan gully so far. Figure 13 and  
516 Figure 14 indicated that the only 5 debris flow events all triggered by the rainfalls with  
517 high-intensity and short-duration. In the future, the value of the curve should be further vali-  
518 dated and continuously corrected with more rainfall and disaster data in later years.

## 519 **6 Conclusions**

520 (1) In the Wenchuan earthquake affected areas, loose deposits are widely distributed,  
521 causing dramatic changes on the environmental development for the occurrence of debris  
522 flow; thus, the debris flow occurrence increased dramatically in the subsequent years. The

523 characteristics of the 10-min, 1-h and 24-h critical rainfalls were represented based on a com-  
524 prehensive analysis of limited rainfall and hazards data. The statistical results show that the  
525 10-min and 1-h critical rainfalls of different debris flow events have minor differences; how-  
526 ever, the 24 hour critical rainfalls vary widely. The 10-min and 1-h critical rainfalls have a no-  
527 tably higher correlation with debris flow occurrences than to the 24-h critical rainfalls.

528 (2) The rainfall pattern of the Guojuanyan gully is the peak pattern, both single peak and  
529 multi-peak. The antecedent precipitation index ( *API* ) was fully explored by the antecedent  
530 effective rainfall and triggering rainfall.

531 (3) As an important and effective means of debris flow early warning and mitigation, the  
532 rainfall threshold of debris flow was determined in this paper, and a new method to calculate  
533 the rainfall threshold is put forward. Firstly, the rainfall characteristics, hydrological charac-  
534 teristics, and some other topography conditions were analyzed. Then, the critical water depth  
535 for the initiation of debris flows is calculated according to the topography conditions and  
536 physical characteristics of the loose solid materials. Finally, according to the initiation mecha-  
537 nism of hydraulic-driven debris flow, combined with the runoff yield and concentration laws  
538 of the watershed, this study promoted a new method to calculate the debris flow rainfall  
539 threshold. At last, the hydrological condition for the initiation of a debris flow is the result of  
540 both short-duration heavy rains (  $I_{60}$  ) and the antecedent precipitation index ( *API* ). The  
541 proposed approach resolves the problem of debris flow early warning in areas with scarcity  
542 data, can be used to establish warning systems of debris flows for similar catchments in areas  
543 with scarcity data although it still need further modification. This study provides a new  
544 thinking for the debris flow early warning in the mountain areas.

## 545 **Acknowledgments**

546 This paper is supported by the CRSRI Open Research Program (Program No:  
547 CKWV2015229/KY), National Key R&D Program of China (2017YFC1502502), CAS Pioneer  
548 Hundred Talents Program, and National Nature Science Foundation of China (No. 41372331 ,  
549 No. 41672318 & No.51679229).

## 550 **References**

551 Althuwaynee OF, Pradhan B, Ahmad N (2015) Estimation of rainfall threshold and its use in landslide hazard  
552 mapping of Kuala Lumpur metropolitan and surrounding areas. *Landslides* 12:861-875.  
553 doi:10.1007/s10346-014-0512-y

554 Bai LP, Sun JL, Nan Y (2008) Analysis of the critical rainfall thresholds for mudflow in Beijing, China. *Geological*  
555 *Bulletin of China* 27(5): 674-680.(in Chinese)

556 Baum RL, Godt JW (2010). Early warning of rainfall-induced shallow landslides and debris flows in the USA.  
557 *Landslides*, 7(3):259–272.

558 Bogaard, T. and Greco, R.(2018) Invited perspectives: Hydrological perspectives on precipitation intensity-duration  
559 thresholds for landslide initiation: proposing hydro-meteorological thresholds, *Nat. Hazards Earth Syst. Sci.*, 18,  
560 31–39, <https://doi.org/10.5194/nhess-18-31-2018>

561 Caine, N (1980) The rainfall intensity-duration control of shallow landslides and debris flows. *Physical Geography*  
562 62A (1-2):23-27

563 Campbell RH (1975) Debris Flow Originating from Soil Slip during Rainstorm in Southern California. *Q. Engineering*  
564 *Geologist*7: 339–349. DOI:10.1144/GSL.QJEG.1974.007.04.04

565 Canli, E., Mergili, M., and Glade, T.(2017) Probabilistic landslide ensemble prediction systems: Lessons to be learned  
566 from hydrology, *Nat. Hazards Earth Syst. Sci. Discuss.*, <https://doi.org/10.5194/nhess-2017-427>, in review

567 Cannon, Susan H., et al.(2008) Storm rainfall conditions for floods and debris flows from recently burned areas in  
568 southwestern Colorado and southern California. *Geomorphology* 96(3): 250-269.

569 Cao Z., Pender G., Wallis S., Carling P.(2004) Computational dam-break hydraulics over erodible sediment bed.  
570 *Journal of hydraulic engineering* 130.7 (2004): 689-703.

571 Chen, Su-Chin, and Bo-Tsung Huang (2010) Non-structural mitigation programs for sediment-related disasters after  
572 the Chichi Earthquake in Taiwan. *Journal of Mountain Science* 7(3): 291-300.

573 Chen YS (2008) An influence of earthquake on the occurrence of landslide and debris flow. Taipei: National Cheng  
574 Kung University.

575 Chen YJ, Yu B, Zhu Y, et al. (2013) Characteristics of critical rainfall of debris flow after earthquake - a case study of  
576 the Xiaogangjian gully. *Journal of Mountain Science* 31(3): 356-361. (in Chinese)

577 Cheng ZL, Zhu PY, Liu LJ (1998) The Relationship between Debris Flow Activity and Rainfall Intensity. *Journal of*  
578 *Natural Disasters*7 (1): 118–120. (in Chinese)

579 Chen NS, Yang CL, Zhou W, et al. (2009) The Critical Rainfall Characteristics for Torrents and Debris Flows in the  
580 Wenchuan Earthquake Stricken Area. *Journal of Mountain Science* 6: 362-372. DOI: 10.1007/s11629-009-1064-9

581 Cui P (1991) Experiment Research of the Initial Condition and Mechanism of Debris Flow. *Chinese Science Bulletin*  
582 21:1650–1652. (in Chinese)

583 Cui P, Hu KH, Zhuang JQ Yang Y, Zhang J (2011) Prediction of debris-flow danger area by combining hydro-logical  
584 and inundation simulation methods. *Journal of Mountain Science* 8(1): 1-9. doi: 10.1007/s11629-011-2040-8

585 Cui P, Zhu YY, Chen J, et al. (2007) Relationships between antecedent rainfall and debris flows in Jiangjia Ravine,  
586 China. In: Chen C L and Majir JJ (eds.), *Debris flow hazard mitigation mechanics, Prediction, and Assessment*.  
587 Millpress, Rotterdam: 1-10.

588 Dahal RK, Hasegawa S, Nonomura A, et al. (2009) Failure characteristics of rainfall-induced shallow landslides in

589 granitic terrains of Shikoku Island of Japan. *Environmental geology* 56(7): 1295-1310. DOI:  
590 10.1007/s00254-008-1228-x

591 Degetto M, Gregoretti C, Bernard M (2015) Comparative analysis of the differences between using LiDAR  
592 contour-based DEMs for hydrological modeling of runoff generating debris flows in the Dolomites. *Front. Earth Sci.*  
593 3, 21. doi: 10.3389/feart.2015.00021

594 **Frattini P, Crosta G, Sosio R (2009) Approaches for defining thresholds and return periods for rainfall - triggered**  
595 **shallow landslides. *Hydrol Proc* 23(10):1444-1460. doi:10.1002/hyp.7269**

596 Gregoretti C, Degetto M, Boreggio M (2016) GIS-based cell model for simulating debris flow runout on a fan. *Journal*  
597 *of Hydrology* 534: 326-340. doi: 10.1016/j.jhydrol.2015.12.054

598 Guido Rianna, Luca Pagano, Gianfranco Urciuoli (2014) Rainfall patterns triggering shallow flowslides in pyroclastic  
599 soils. *Engineering Geology*, 174: 22-35 doi: 10.1016/j.enggeo.2014.03.004

600 Guo, X.J., Cui, P., Li, Y., 2013. Debris flow warning threshold based on antecedent rainfall: a case study in Jiangjia  
601 Ravine, Yunnan, China. *J. Mt. Sci.* 10 (2), 305–314.

602 Guzzetti, F., Peruccacci, S., Rossi, M., & Stark, C. P. (2008). The rainfall intensity–duration control of shallow  
603 landslides and debris flows: an update. *Landslides*, 5(1), 3-17.

604 Hu M J, Wang R (2003) Testing Study of the Correlation among Landslide, Debris Flow and Rainfall in Jiangjia Gully.  
605 *Chinese Journal of Rock Mechanics and Engineering*, 22(5): 824–828 (in Chinese)

606 Hong Y, Hiura H, Shino K, et al. (2005) The influence of intense rainfall on the activity of large-scale crystalline schist  
607 landslides in Shikoku Island, Japan. *Landslides* 2(2): 97-105. DOI: 10.1007/s10346-004-0043-z

608 Hu W, Dong XJ, Wang GH, van Asch TWJ, Hicher PY (2016) Initiation processes for run-off generated debris flows  
609 in the Wenchuan earthquake area of China. *Geomorphology* 253: 468–477. doi: 10.1016/j.geomorph.2015.10.024

610 Iverson RM, Lahusen RG (1989) Dynamic Pore-Pressure Fluctuations in Rapidly Shearing Granular Materials.  
611 *Science* 246 (4931): 796–799. DOI: 10.1126/science.246.4931.796

612 Jianqi Zhuang, Peng Cui, Gonghui Wang, et al. (2015) Rainfall thresholds for the occurrence of debris flows in the  
613 Jiangjia Gully, Yunnan Province, China. *Engineering Geology*, 195: 335-346.

614 **Jiang X., Cui P., Chen H., Guo Y. (2016) Formation conditions of outburst debris flow triggered by overtopped natural**  
615 **dam failure. *Landslides* 14(3):1-11.**

616 Jibson RW (1989) Debris flows in southern Puerto Rico. *Geological Society of America Special Papers* 236: 29-56.  
617 DOI: 10.1130/SPE236-p29

618 Jun Wang, Shun Yang, Guoqiang Ou, et al. (2017) Debris flow hazards assessment by combining numerical simulation  
619 and land utilization. *Bulletin of Engineering Geology and the Environment*, 1-15. Doi: 10.1007/s10064-017-1006-7

620 **Lagomarsino D, Segoni S, Rosi A, Rossi G, Battistini A, Catani F, Casagli N (2015) Quantitative comparison between**  
621 **two different methodologies to define rainfall thresholds for landslide forecasting. *Nat Hazards Earth Syst Sci***  
622 **15:2413–2423. doi:10.5194/nhess-15-2413-2015**

623 Liang GM, Yao LK (2008) Study on the critical rainfall for debris flows. *Lu Ji Gongcheng* 6: 3-5. (in Chinese)

624 Liu YH, Tang C, Li TF, et al. (2009) Statistical relations between geo-hazards and rain type. *Journal of Engineering*  
625 *Geology* 17(5): 656-661. (in Chinese)

626 Liu JF, You Y, Chen XZ, Fan JR (2010) Identification of potential sites of debris flows in the upper Min River  
627 drainage, following environmental changes caused by the Wenchuan earthquake. *Journal of Mountain Science* 3:  
628 255-263. doi: 10.1007/s11629-010-2017-z

629 Lanzoni, S., C. Gregoretti, and L. M. Stancanelli (2017) Coarse-grained debris flow dynamics on erodible beds, *J. Ge-*  
630 *ophys. Res. Earth Surf.*, 122, doi:10.1002/2016JF004046.

631 McCoy SW, Kean JW, Coe JA, Tucker GE, Staley DM, Wasklewicz WA (2012) Sediment entrainment by debris flows:  
632 In situ measurements from the head waters of a steep catchment. *J. Geophys. Res.*117, F03016. doi:  
633 10.1029/2011JF002278

634 Mohamad Ayob Mohamadi, Ataollah Kavian (2015) Effects of rainfall patterns on runoff and soil erosion in field plots.  
635 *International Soil and Water Conservation Research* 3: 273-281.  
636 <http://dx.doi.org/10.1016/j.iswcr.2015.10.001>Imaizumi F, Sidle RC, Tsuchiya S, Ohsaka O (2006)  
637 Hydrogeomorphic processes in a steep debris flow initiation zone. *Geophys. Res. Lett.* 33, L10404. doi:  
638 10.1029/2006GL026250

639 Pan HL, Ou GQ, Hang JC, et al.(2012)Study of rainfall threshold of debris flow forewarning in data lack areas. *Rock*  
640 *and Soil Mechanics* 33(7): 2122-2126. (in Chinese)

641 Pan HL, Huang JC, Wang R, et al. (2013) Rainfall Threshold Calculation Method for Debris FlowPre-Warning in  
642 Data-Poor Areas. *Journal of Earth Science* 24(5): 854–862. DOI:10.1007/s12583-013-0377-3

643 Rosi A, Lagomarsino D, Rossi G, Segoni S, Battistini A, Casagli N (2015) Updating EWS rainfall thresholds for the  
644 triggering of landslides. *Nature Hazard* 78:297–308

645 Saito H, Nakayama D, Matsuyama H (2010) Relationship between the initiation of a shallow landslide and rainfall  
646 intensity—duration thresholds in Japan. *Geomorphology* 118(1): 167-175. DOI: 10.1016/j.geomorph.2009.12.016

647 Sassa, K., Nagai, O., Solidum, R., Yamazaki, Y., & Ohta, H. (2010) An integrated model simulating the initiation and  
648 motion of earthquake and rain induced rapid landslides and its application to the 2006 Leyte landslide. *Landslides*,  
649 7(3), 219-236.

650 Segoni S, Battistini A, Rossi G, Rosi A, Lagomarsino D, Catani F, Moretti S, Casagli N (2015) Technical note: an  
651 operational landslide early warning system at regional scale based on space–time variable rainfall thresholds. *Nat*  
652 *Hazards Earth Syst Sci* 15: 853–861

653 Segoni S, Rosi A, Lagomarsino D, Fanti R, and Casagli N (2018) Brief Communication: Using averaged soil moisture  
654 estimates to improve the performances of a regional-scale landslide early warning system. *Nat. Hazards Earth Syst.*  
655 *Sci.*

656 Shied CL, Chen LZ (1995) Developing the critical line of debris –flow occurrence. *Journal of Chinese Soil and Water*  
657 *Conservation* 26(3):167-172. (in Chinese)

658 Shieh CL, Chen YS, Tsai YJ, et al (2009) Variability in rainfall threshold for debris flow after the Chi-Chi earthquake  
659 in central Taiwan, China. *International Journal of Sediment Research* 24(2): 177-188.

660 Staley, D.M., Kean, J.W., Cannon, S.C., Schmidt, K.M., Laber, J.L. (2013) Objective definition of rainfall  
661 intensity–duration thresholds for the initiation of post-fire debris flows in southern California, *Landslides* 10,  
662 547–562

663 Takahashi T (1978) Mechanical Characteristics of Debris Flow. *Journal of the Hydraulics Division* 104:1153–1169

664 Tang C, Zhu J, Li WL (2009) Rainfall-triggered debris flows following the Wenchuan earthquake. *Bull Eng Geol*  
665 *Environ* 68(2):187–194. DOI: 10.1007/s10064-009-0201-6

666 Tang C, Van Asch TWJ, Chang M, et al.(2012) Catastrophic debris flows on 13 August 2010 in the Qingping area,  
667 southwestern China: the combined effects of a strong earthquake and subsequent rainstorms.  
668 *Geomorphology* 139–140:559–576. DOI: 10.1016/j.geomorph.2011.12.021

669 Tang C, Zhu J, Chang M, et al. (2012) An empirical–statistical model for predicting debris-flow runout zones in the  
670 Wenchuan earthquake area. *Quaternary International* 250:63–73. DOI:10.1016/j.quaint.2010.11.020.

671 Tecca PR, Genevois R (2009) Field observations of the June 30, 2001 debris flow at Acquabona (Dolomites, Italy).  
672 *Landslides* 6(1): 39-45. doi: 10.1007/s10346-009-0145-8

673 Tian B, Wang YY, Hong Y (2008) Weighted relation between antecedent rainfall and process precipitation in debris  
674 flow prediction—A case study of Jiangjia gully in Yunnan province. *Bulletin of Soil and Water Conservation* 28(2):  
675 71-75.(in Chinese)

676 Tiranti D, Deangeli C (2015) Modeling of debris flow depositional patterns according to the catchment and sediment  
677 source area characteristics. *Front. Earth Sci.* 3, 8. doi: 10.3389/feart.2015.00008

678 Tofani et al., Soil characterization for shallow landslides modeling: a case study in the Northern Apennines (Central  
679 Italy). 2017. *Landslides* 14:755–770, DOI 10.1007/s10346-017-0809-8

680 Y.Zhao, F. Wei, H.Yang, et al. (2011) Discussion on Using Antecedent Precipitation Index to Supplement Relative Soil  
681 Moisture Data Series. *Procedia Environment Sciences* 10: 1489-1495.

682 Wang EC, Meng QR (2009) Mesozoic and cenozoic tectonic evolution of the Longmenshan fault belt. *Science in China*  
683 *Series D: Earth Sciences* 52(5): 579-592. DOI:10.1007/s11430-009-0053-8

684 Wang G., Furuya G., Zhang F., Doi I., Watanabe N. (2016) Layered internal structure and breaching risk assessment  
685 of the Higashi-Takezawa landslide dam in Niigata, Japan. *Geomorphology*, 267:48-58.

686 Wang J, Ou GQ, Yang S, Lu GH, et al. (2013) Applicability of geomorphic information entropy in the post-earthquake  
687 debris flow risk assessment. *Journal of Mountain Science* 31(1): 83-91. (in Chinese)

688 Wang J, Yu Y, Yang S, et al.(2014) A Modified Certainty Coefficient Method (M-CF) for Debris Flow Susceptibility  
689 Assessment: A Case Study for the Wenchuan Earthquake Meizoseismic Areas. *Journal of Mountain Science* 11(5):  
690 1286-1297. DOI: 10.1007/s11629-013-2781-7.

691 Wang J, Yu Y, Ou GQ, et al.(2016) Study on the Geotechnical Mechanical Characteristics of Loose Materials in the  
692 Wenchuan Earthquake-hit Areas. *Science Technology and Engineering* 16(5): 11-18. (in Chinese)

693 Wieczorek GF (1987) Effect of rainfall intensity and duration on debris flows in central Santa Cruz Mountain, California.  
694 *Engineering Geology* 7: 93-104. DOI: 10.1130/REG7-p93

695 Wilson, RC, Jayko AS (1997) Preliminary Maps Showing Rainfall Thresholds for Debris-Flow Activity, San  
696 Francisco Bay Region, California. U.S. Geological Survey Open-File Report 97-745 F

697 Winter, M. G., et al. (2010) Debris flow, rainfall and climate change in Scotland. *Quarterly Journal of Engineering*  
698 *Geology and Hydrogeology* 43(4): 429-446.

699 Xu ZQ, Ji SC, Li HB, et al. (2008) Uplift of the Longmen Shan range and the Wenchuan earthquake. *Episodes* 31(3):  
700 291-301

701 Xu Q, Zhang S, Li WL, et al.(2012) The 13 August 2010 catastrophic debris flows after the 2008 Wenchuan earthquake,

702 China. *Natural hazards and earth system sciences* 12(1):201–216. DOI: 10.5194/nhess-12-201-2012

703 Yao LK (1988) A research on the calculation of critical rainfall with frequency of debris flow and torrential rain.

704 *Journal of Soil and Water Conservation* 2(4): 72-78 (in Chinese)

705 Ye SZ (1992) *Hydrological calculation*. Water conservancy and Hydropower Press, 111.

706 Zhou, W., & Tang, C. (2014). Rainfall thresholds for debris flow initiation in the Wenchuan earthquake-stricken area,

707 southwestern China. *Landslides*, 11(5), 877-887.

708 Zhuang JQ, Cui P, Ge YG, et al. (2009) Relationship between rainfall characteristics and total amount of debris flow.

709 *Journal of Beijing Forestry University* 31(4): 77-83 (in Chinese)

710 Zhang SJ, Yang HJ, Wei FQ, et al. (2014) A Model of Debris Flow Forecast Based on the Water-Soil Coupling

711 Mechanism. *Journal of Earth Science*, 25(4): 757-763. DOI:10.1007/s12583-014-0463-1

712 Zhenlei Wei, Yuequan Shang, Yu Zhao, et al. (2017) Rainfall threshold for initiation of channelized debris flows in a

713 small catchment based on in-site measurement. *Engineering Geology*, 217, 23-34.